JJEES

Volume 2, (Special Publication, Number 1), December. 2009
ISSN 1995-6681
Pages 60- 65

Jordan Journal of Earth and Environmental Sciences

Exchange Coupling and Magnetic Properties of Fe/Ir(001) superlattices

B. Alqassem, B.A. Hamad*, J.M. Khalifeh

Department of Physics, University of Jordan, Amman 11942, Jordan

Abstract

We present ab initio calculations of the exchange coupling for Fe/Ir system using a self-consistent full-potential linearized augmented plane-wave (FLAPW) method. The local spin density approximation (LSDA) as well as the generalized gradient approximation (GGA) are used to treat the exchange correlation potential. In this work, supercells consisting of two layers of Fe separated by Ir layers ranging from 1 to 7 are constructed. For each spacer layer thickness, two calculations were performed, one for ferro- and another for anti-ferromagnetic ordering of Fe atoms. We obtained an oscillatory behavior for the interlayer exchange coupling with a period of 7.83 Å for both LSDA as well as GGA.

Keywords: Magnetism, Superlattice, Fe, Ir, Exchange Coupling, ab initio calculations.

1. Introduction

All through the last two decades, the influence of interlayer exchange coupling (IEC) between magnetic layers separated by a non-magnetic spacer has involved substantial efforts. Ever since, it was firstly studied by Grünberg [1] for Fe/Cr superlattices in 1986, and following the discovery of Parkin [2] on coupling oscillates between the FM and the AF configurations as a function of spacer layer thickness, and the inertest is on the rise. Shortly afterwards, Parkin has shown that oscillatory exchange coupling occurs with almost all transition and noble metals as spacer materials [3]. Not until the last decade when the reward of this detection is translated to a definite application. The giant magneto-resistance became a renowned industrial application for the coupling. The giant magneto-resistances are utilized as responsive detectors for magnetic field in magnetic data storage; it is now commonly used in magnetic read head of all magnetic recording devices. It is all due to the remarkable properties of these materials, exhibited in the great change of their resistance once placed in a small field, large enough to reverse their magnetic alignments. This discovery gave an important momentum for intensive investigations in this area of research [4-11].

An assortment of methodologies covering a wide spectrum of theoretical approaches has been explored to clarify this inspiring phenomenon, approaches like the first principles or tight-binding total energy calculations [12-15], the Ruderman-Kittel- Kasuya-Yosida (RKKY) theory [16-19], a free-electron model [20-22] and the Anderson s-d Mixing models [23, 24]. Recently, a new disclosure stating that every one of the above models can be integrated into a more broad approach. Seeing the interlayer

-exchange coupling as an interpretation of quantum size effect and described in terms of

(spin-dependent) reflection coefficients of electrons at the interfaces between the nonmagnetic spacer and the ferromagnetic layers [25-27].

In this work, we study the interlayer exchange coupling in Fe/Ir(001) superlattices using a self-consistent full-potential linearized augmented plane-wave (FLAPW) method. Although, this system is expected to be a good candidate for interlayer exchange coupling, yet the theoretical studies to investigate its behavior are scarce. Previous experimental studies have obtained high quality of Fe/Ir(001) superlattice with flat interfaces and absence of interdiffusion [28-30], the fact that makes them promising structures for GMR devices.

The rest of the paper is arranged as follows: In section, II we present the computational details of calculations; in section III, we put forward the results and discussion; and finally, in section IV we provide recommendations and conclusions.

* Corresponding author. b.hamad@ju.edu.jo

  - Volume 2, (Special Publication, Number 1)(ISSN 1995-6681)

2. Computational Details

All calculations are performed using the self-consistent full-potential linearized augmented plane-wave (FLAPW) method within the density functional theory [31]. The calculations are carried out using the LSDA [32] as well as GGA [33] approximations. The cutoff energy of the plane waves in the interstitial region between the muffin tins is taken as 16 Ry for the wavefunction and 169 Ry for the potential. The k-point sampling is performed using Monkhorst–Pack grid in the irreducible part of the Brillouin zone. The wavefunction expansion inside the muffin tins are taken up to lmax = 10 and the potential expansion up to lmax = 4. These parameters were chosen to set the self-consistent calculations where the convergence is taken with respect to the total charge of the system with a tolerance of 0.0001 electron charges. The muffin-tin radii are taken to be 1.12 Å and 1.24 Å for Fe and Ir, respectively. The calculations are performed using Fermi-level smearing of 0.005 Rydberg.

The calculated lattice constant of bulk ground states of bcc Fe and fcc Ir are found to be 2.84 Å and 3.87 Å. We used the supercell technique to build FeIrn (n=1-7) superlattices, Fig.1 presents one of these supercells, namely FeIr4 superlattice. To optimize the structures, the lattice constants for each cell were relaxed in three steps. We start with a cubic supercell and varying the volume of the supercell keeping the c/a ratio constant. The energy dependence on the volume is tested and the equilibrium volume is obtained using the Murnaghan's equation of state fit [34]. Then varying the c/a ratio at the equilibrium volume obtained from the first step. The energy dependence on the c/a ratio is tested to obtain the equilibrium value. Finally, the volume of the supercell re-varied again at the equilibrium c/a ratio obtained from the second step. The new equilibrium volume is found by the Murnaghan's equation of state fit [34].

The lattice constants for each superlattice structure are given in Table 1. It is to be noted here that the lattice parameters are compared with those obtained by Vegard's law [35], where the lattice constants are calculated using the following equations:

$$a = \frac{a_{Fe} + n a_{Ir}/\sqrt{2}}{n+1} \quad (1)$$

$$c = \sqrt{2}a\left(\frac{n+1}{2}\right) \quad (2)$$

here the $\sqrt{2}$ factor is used to convert from fcc-structure to bct-structure, while the $(n+1)/2$ factor represents the number of unit cells formed. A close look at Table 1 reveals that the lattice constants of the supercells obtained by the optimization technique are close to those of Vegard's law.

The total energy is calculated for ferro- and antiferromagnetic configurations of Fe for each $FeIr_n$ superlattice. The same structure has been used for both configurations for the sake of consistency to obtain reliable energy differences, i.e. the unit cell is doubled even in the ferromagnetic configuration for comparison purposes. The exchange coupling, *j*, is calculated using the equation:

$$j(d) = E_{tot}^{\uparrow\downarrow}(d) - E_{tot}^{\uparrow\uparrow}(d) \quad (3)$$

where *d* is the thickness of the spacer layer and $E_{tot}^{\uparrow\downarrow}(d)$ and $E_{tot}^{\uparrow\uparrow}(d)$ are the total energies of the system in AF and FM arrangements. The exchange

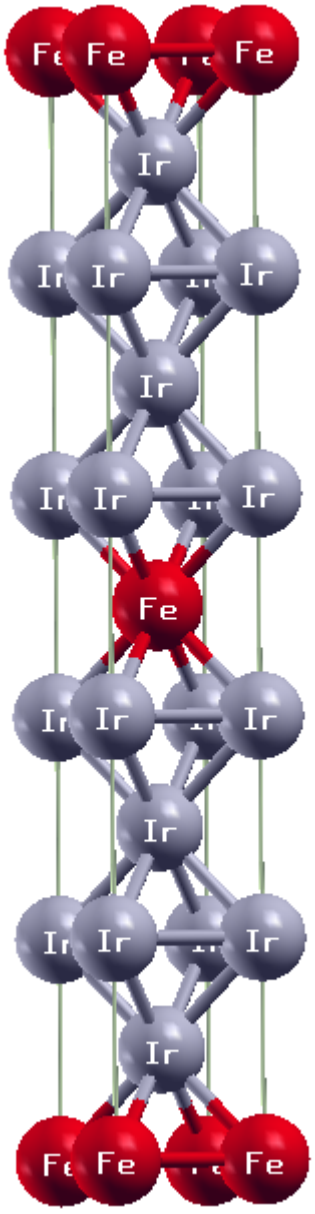

Fig.1 : The schematic diagram for $FeIr_4$ supercell.

coupling convergence with respect to the number of k-points in the irreducible Brillouin zone (IBZ) has been checked for each $FeIr_n$ structure. The convergence test of *j* as a function of the number of *k* points is shown in Fig. 2 for both the LSDA and GGA exchange potentials. It is found that *j* converges faster than the total energy as a function of the number of k-points.

3. Results and Discussion

3.1. Exchange Coupling

The study of the interlayer exchange coupling requires the calculation of the total energy of Ferro- and antiferromagnetic ordering of Fe designed for each Ir spacer layer thickness. The IEC is calculated for both LSDA and GGA exchange correlation potentials as shown in Fig. 3. As the Ir spacer thickness is increased, the IEC oscillate between FM and AF by a period of oscillation about 7.83 Å for both the LSDA and GGA potentials, which is comparable with that obtained by Stoeffler [36]. It is to be noted here that only one period of oscillation could be obtained in our calculations since we are restricted with small Ir thickness up to 14 Å.

From Fig.3, it can be noticed that the LSDA calculations give higher values of the interlayer exchange coupling than those obtained using the GGA exchange-correlation potential, with the same period of oscillation for both approximations.

Table1:The lattice constants for the relaxed seven superlattices.

Superlattice	*Lattice Constants by Optimization Technique*		*Lattice Constants by Vegard's Law*	
	a (Å)	c (Å)	a (Å)	c (Å)
$FeIr$	2.67	3.64	2.79	3.94
$FeIr_2$	2.71	5.60	2.77	5.88
$FeIr_3$	2.71	7.62	2.76	7.81
$FeIr_4$	2.72	9.56	2.76	9.75
$FeIr_5$	2.73	11.45	2.75	11.68
$FeIr_6$	2.73	13.42	2.75	13.62
$FeIr_7$	2.73	15.40	2.75	15.55

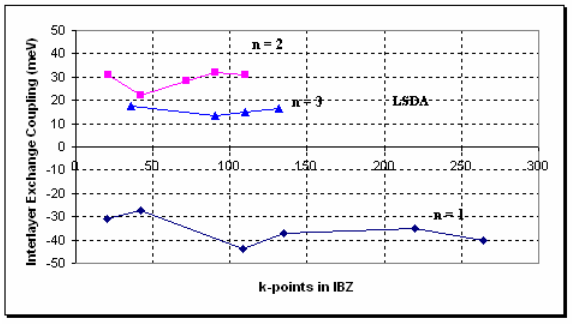

(*a*)

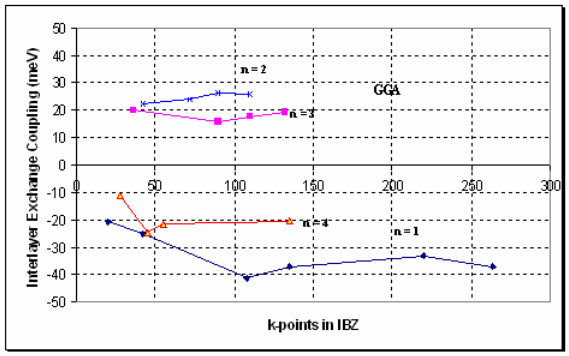

(*b*)

Fig. 2 : Interlayer exchange coupling, *j*(meV) for $FeIr_n$ multilayers as a function of the number of **k**- points in the IBZ for different number of Ir layers for (a) LSDA and (b) GGA.

3.2. Magnetic structure

Magnetic moments (in Bohr magnetons, μ_B) for the case of FM ordering, using the GGA and LSDA calculations for different layers, are presented in Table 2 and Table 3, respectively. As expected, the Fe layer carries the overwhelming part of the total magnetic moment. The table also points out the following: (i) the first Ir substrate layer continuously ferromagnetically coupled to the Fe layer. (ii) The second Ir layer continually antiferromagnetically coupled to the Fe layer.

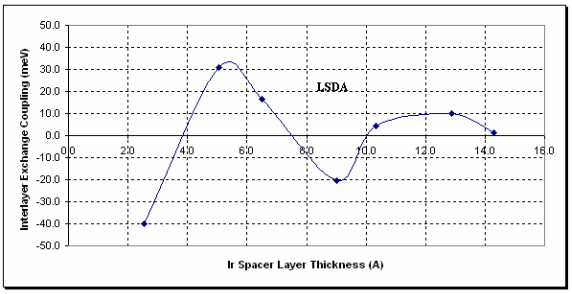

(*a*)

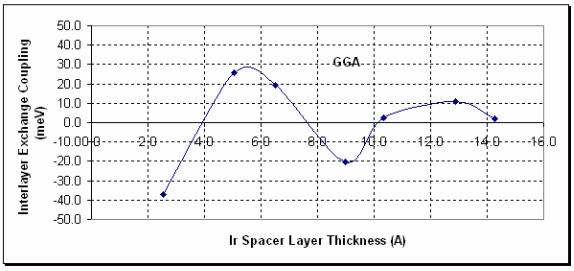

(*b*)

Fig. 3: Interlayer exchange coupling, (meV) for $FeIr_n$ multilayers as a function of Ir spacer layer thickness (Å) for (a) LSDA and (b) GGA potentials.

Table 2: Magnetic moments (in Bohr magnetons) for each layer in the Fe/Ir unit cell using the GGA approximation. Results are shown for one Fe layer on top of up to 7 Ir layers.

	Ir layer number						
Fe	1	2	3	4	5	6	7
2.14536	0.03033						
2.52453	-0.07337	-0.07338					
2.68122	0.08753	-0.10992	0.08690				
2.69386	0.09129	-0.04400	-0.04406	0.09129			
2.68806	0.04772	-0.06590	0.00860	-0.06586	0.04770		
2.70738	0.05870	-0.07538	0.00964	0.00966	-0.07516	0.05875	
2.72556	0.07470	-0.05586	0.00494	0.02015	0.00497	-0.05588	0.07471

In Fig. 4, the induced magnetic moments per atom on the Ir spacer layers are plotted, using both the GGA as well

as the LSDA potentials, for the $FeIr_7$ multilayers system. The induced magnetic moments of Ir atoms are oscillating; however, the magnetic moments in the central layers are weaker than those at the interface. The induced magnetic moment at the interface is 0.075 μ_B whilst 0.020 μ_B at the central layer for the GGA calculations. The induced magnetic moments are reduced in the LSDA calculations. The induced magnetic moment at the interface is 0.056 μ_B whilst 0.017 μ_B at the middle layer.

Table 3: Magnetic moments (in Bohr magnetons) for each layer in the Fe/Ir unit cell using the LSDA approximation. Results are shown for one Fe layer on top of up to 7 Ir layers.

	Ir layer number						
Fe	1	2	3	4	5	6	7
1.93343	0.02476						
2.32311	-0.06518	-0.06518					
2.51308	0.07706	-0.09588	0.07706				
2.51253	0.06905	-0.03793	-0.03794	0.06906			
2.51602	0.03807	-0.05674	0.00828	-0.05674	0.03807		
2.54075	0.04495	-0.06511	0.01152	0.01152	-0.06511	0.04495	
2.55823	0.05584	-0.05095	0.00593	0.01701	0.00593	-0.05104	0.05584

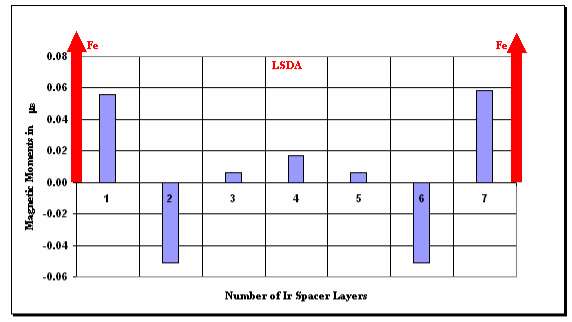

(a)

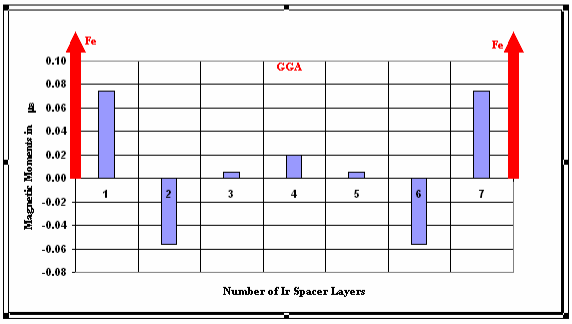

(b)

Fig. 4: Induced magnetic moments on Ir apacer layer in ferromagnetic $FeIr_7$ multilayer using (a) LSDA and (b) GGA calculations. The Fe atoms are placed in positions 0 and 8.

The oscillatory behavior also appears for the magnetic moments on Ir atoms, with zero magnetic moment at the central Ir atom, Fig.5.

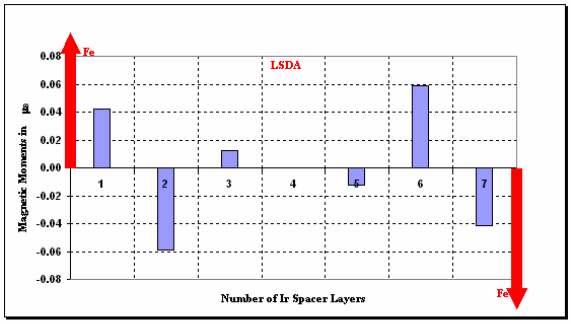

(a)

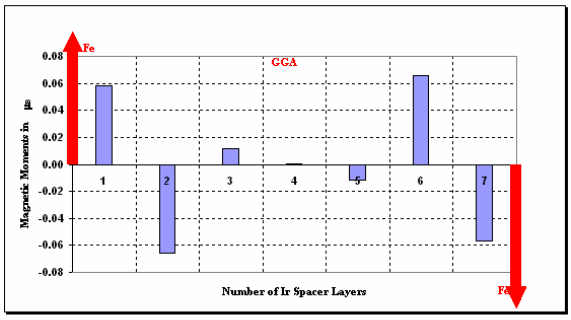

(b)

Fig. 5: Induced magnetic moments on Ir apacer layer in anti-ferromagnetic $FeIr_7$ multilayer using (a) LSDA and (b) GGA calculations. The Fe atoms are placed in positions 0 and 8.

4. Conclusion

The IEC for Fe/Ir is calculated by using the self-consistent FLAPW method with the LSDA and GGA exchange correlation potentials. We can summarize the main points of this study as follows:

1. The IEC has an oscillatory behavior as a function of Ir spacer layer thickness with a period of 7.83 Å for both the LSDA as well as the GGA potentials. The period of oscillation is found to be the same for both the LSDA as well as GGA potentials.
2. The induced magnetic moments on Ir atoms show an oscillatory behavior. The first Ir substrate layer is always ferromagnetically coupled to the magnetic layer, whereas, the interior Ir layers are coupled antiferromagnetically.
3. The GGA gives higher magnetic moments for Fe and Ir as compared to the LSDA.

References

[1] P. Grünberg, R. Schreiber, Y. Pang, M. B. Brodsky, and H. Sowers, Phys. Rev. Lett., 57, 2442 (1986).

[2] S. S. P. Parkin, N. More, and K. P. Roche. Phys. Rev. Lett. 64, 2304(1990).

[3] S. S. P. Parkin Phys. Rev. Lett. 67, 3598 (1991).

[4] Dinia, M. Stoeffel, K. Rahmouni, and D. Stoeffler, Europhys.Lett. 42, 331 (1998).

[5] H. Yanagihara, Eija Kita, and M. B. Salamon, Phys. Rev. B 60,12957 (1999).

[6] Y. Lou, M. Moske, and K. Samwer, Europhys. Lett. 42, 565 (1998).

[7] S. Colis, A. Dinia, C. Ulhaq-Bouillet, P. Panissod, C. Meny, G.Schmerber, and J.Arabski, Phys. Stat. Sol. (a) 199, 161 (2003).

[8] S. Mirbt, O. Eriksson, B. Johansson, and H. L. Skriver, Phys. Rev.B 52, 15070 (1995).

[9] S. Mirbt, A. M. N. Niklasson, B. Johansson, and H. L. Skriver, Phys. Rev. B 54, 6382 (1996).

[10] J. Unguris, R. J. Celotta, and D. T. Pierce, Phys. Rev. Lett. 79, 2734 (1997).

[11] N. N. Shukla and R. Prasad, Phys. Rev. B 70, 14420 (2004).

[12] F. Herman, J. Sticht, and M. V. Schilfgaarde. J. Appl. Phys. 69, 4783 (1991).

[13] P. Lang, L. Nordström, R. Zeller, and P. H. Dederichs, Phys. Rev. Lett. 71, 1927 (1993).

[14] J. Kudrnovský, V. Drchal, L. Turek, and P. Weinberger, Phys. Rev. B 50, 16105 (1994).

[15] D. Stoeffler and F. Gautier, Phys. Rev. B 44, 10389 (1991).

[16] Y. Yafet, Phys. Rev. B 36, 3948 (1987).

[17] [17] C. Chappert and J. P. Renard, Europhys. Lett. 15, 553 (1991).

[18] W. Baltensperger and J. S. Helman, Appl. Phys. Lett. 57, 2954 (1990).

[19] R. Coehoorn, Phys. Rev. B 44, 9331 (1991).

[20] J. Barnas, J. Magn. Magn. Mater. 111, L215 (1992).

[21] R. P. Erickson, K. B. Hathaway, and J. R. Cullen, Phys. Rev. B 47, 2626 (1993).

[22] J. C. Slonczewski, J. Magn. Magn. Mater. 126, 374 (1993).

[23] Y. Wang, P. M. Levy and J. L. Fry, Phys. Rev. Lett. 65, 2732(1990).

[24] P. Bruno, J. Magn. Magn. Mater. 116, L13 (1992).

[25] M. D. Stiles, Phys. Rev. B 48 7238 (1993).

[26] P. Bruno, J Magn. Magn. Mater. 121, 248 (1993).

[27] P. Bruno, Phys. Rev. B. 52, 418 (1995).

[28] S. Andrieu, M. Piecuch, L. Hennet, J. Hubsch and E. Snoeck, Europhys. Lett. 26, 189 (1994).

[29] S. Andrieu, E. Snòeck, P. Arcade and M. Piecuch, J. Appl. Phys. 77, 1308(1995).

[30] S. Andrieu , Hubsch , E. Snoeck, H. Fischer and M. Piecuch, J. Magn. Magn. Mater. 148, 6 (1995).

[31] P. Blaha, K. Schwarz, and J. Luitz, Wien2k Package (www.wien2k.at), A Full Potential Linearized Augmented Plane Wave Package for Calculating Crystal Properties (Kalheinz Schwarz, Techn. Universitat Wien, Austria).

[32] U. Von Barth, and L. Hedin. J. Phys. C 5, 1629 (1972).

[33] J. P. Perdew, S. Burke, and M. Ernzerhof. Phys. Rev. Lett. 77, 3865 (1996).

[34] F. D. Murnaghan, Proc. Natl. Acad. Sci. (U.S.A.) 30 244 (1944).

[35] L. Vegard, Z. Phys. 5, 17 (1921).

[36] D. Stoeffler, Eur. Phys. J. B 37, 311 (2004).